cmgh
CELLULAR AND MOLECULAR GASTROENTEROLOGY AND HEPATOLOGY

ORIGINAL RESEARCH

The Food Additive Maltodextrin Promotes Endoplasmic Reticulum Stress–Driven Mucus Depletion and Exacerbates Intestinal Inflammation

F. Laudisi,[1] D. Di Fusco,[1] V. Dinallo,[1] C. Stolfi,[1] A. Di Grazia,[1] I. Marafini,[1] A. Colantoni,[1] A. Ortenzi,[1] C. Alteri,[2] F. Guerrieri,[3] M. Mavilio,[1] F. Ceccherini-Silberstein,[2] M. Federici,[1,4] T. T. MacDonald,[5] I. Monteleone,[6] and Giovanni Monteleone[1]

[1]Department of System Medicine, [2]Department of Experimental Medicine and Surgery, [6]Department of Biomedicine and Prevention, University of Rome Tor Vergata, Rome, Italy; [3]Center for Life NanoScience at Sapienza, Istituto Italiano di Tecnologia, Rome, Italy; [4]Center for Atherosclerosis, Policlinico Tor Vergata, Rome, Italy; [5]Blizard Institute, Barts and The London School of Medicine and Dentistry, Queen Mary University of London, Whitechapel, London, United Kingdom

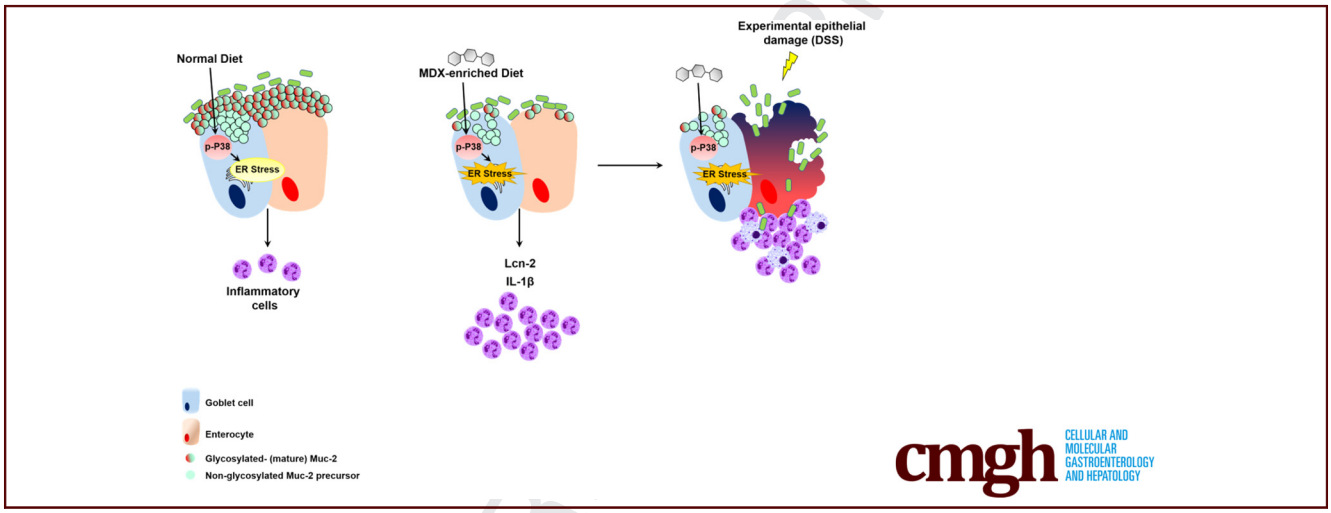

SUMMARY

This study reports that the polysaccharide maltodextrin, which is a common additive used in Western diet for food processing, triggers endoplasmic reticulum stress in goblet cells. Our data support the hypothesis that a Western diet rich in maltodextrin can contribute to gut disease susceptibility and can help design preventive programs for subjects at high risk to develop inflammatory bowel diseases.

BACKGROUND & AIMS: Food additives, such as emulsifiers, stabilizers, or bulking agents, are present in the Western diet and their consumption is increasing. However, little is known about their potential effects on intestinal homeostasis. In this study we examined the effect of some of these food additives on gut inflammation.

METHODS: Mice were given drinking water containing maltodextrin (MDX), propylene glycol, or animal gelatin, and then challenged with dextran sulfate sodium or indomethacin. In parallel, mice fed a MDX-enriched diet were given the endoplasmic reticulum (ER) stress inhibitor tauroursodeoxycholic acid (TUDCA). Transcriptomic analysis, real-time polymerase chain reaction, mucin-2 expression, phosphorylated p38 mitogen-activated protein (MAP) kinase quantification, and H&E staining was performed on colonic tissues. Mucosa-associated microbiota composition was characterized by 16S ribosomal RNA sequencing. For the in vitro experiments, murine intestinal crypts and the human mucus-secreting HT29-MTX cell line were stimulated with MDX in the presence or absence of TUDCA or a p38 MAP kinase inhibitor.

RESULTS: Diets enriched in MDX, but not propylene glycol or animal gelatin, exacerbated intestinal inflammation in both models. Analysis of the mechanisms underlying the detrimental effect of MDX showed up-regulation of inositol requiring protein 1β, a sensor of ER stress, in goblet cells, and a reduction of mucin-2 expression with no significant change in mucosa-associated microbiota. Stimulation of murine intestinal crypts and HT29-MTX cells with MDX induced inositol requiring protein 1β via a p38 MAP kinase–dependent mechanism. Treatment of mice with TUDCA prevented mucin-2 depletion and attenuated colitis in MDX-fed mice.

CONCLUSIONS: MDX increases ER stress in gut epithelial cells with the downstream effect of reducing mucus production and

enhancing colitis susceptibility. *(Cell Mol Gastroenterol Hepatol 2018;■:■–■; https://doi.org/10.1016/j.jcmgh.2018.09.002)*

Keywords: Colitis; IBD; Unfolded Protein Response; Intestinal Epithelium.

Inflammatory bowel disease (IBD) is a term used to describe 2 chronic inflammatory disorders of the gut, namely ulcerative colitis and Crohn's disease.[1] Although the etiology of IBD remains unknown, accumulating evidence has suggested that the pathologic process results from an interaction between environmental and genetic factors, which trigger an excessive intestinal immune response against components of the gut microflora.[2,3] In the past decades, there has been an increase in the incidence of IBD in previously low-incidence regions of the world (eg, Asia), coincident with these countries becoming more westernized.[4–7] Epidemiologic studies have indicated that Western dietary factors, particularly those that result in being overweight or obese, can influence the development of IBD.[8,9] However, it remains unclear which dietary factors have a causative role in IBD and how each of these factors may affect intestinal homeostasis.[10,11] A Western diet can shape the intestinal microbiota and promote overgrowth of microorganisms potentially involved in the development of IBD.[12,13] Indeed, mice given a fat-based diet showed increased abundance and activity of *Bilophila wadsworthia* owing to changes in the production of bile acids, and consequently exacerbation of experimental colitis.[12] Another possibility is that Western diet–related elements, such as high dietary salt and saturated fatty acids, can directly target mucosal immune cells and potentate pathogenic responses.[14–16] In addition, diet can have a direct impact on the mucus layer of the gastrointestinal tract.[17,18]

A Western diet also is rich in food additives, which commonly are added as stabilizers, coating materials, or bulking agents in prepackaged foods. Although the US Food and Drug Administration recognizes these dietary elements as safe, their use has been linked to the development of intestinal pathologies in both animals and human beings.[19–23] For example, synthetic dietary emulsifiers polysorbate 80 and carboxymethylcellulose act directly on human microbiota to increase its proinflammatory potential.[19] It also has been shown that the polysaccharide maltodextrin (MDX), which is commonly used as a filler and thickener during food processing, can alter microbial phenotype and host antibacterial defenses. MDX expands the *Escherichia coli* population in the ileum and induces necrotizing enterocolitis in preterm piglets.[24] Nickerson and McDonald[21] reported that MDX increases cellular adhesion of the "adherent and invasive *E coli*" strain and in vivo studies have shown an increased load of cecal bacteria in MDX-fed mice upon oral infection with *Salmonella*, even though MDX by itself did not induce disease.[20]

In this study, we therefore investigated whether food additives used in the Western diet can perturb intestinal homeostasis and exacerbate gut inflammation.

Results

MDX-Enriched Diet Exacerbates Intestinal Inflammation

To investigate whether food additives promote and/or exacerbate intestinal inflammation, wild-type Balb/c mice were exposed to MDX (5%), propylene glycol (PG) (0.5%), and animal gelatin (GEL) (5 g/L) diluted in drinking water. The selected compounds induced neither clinical and histologic signs of intestinal inflammation nor changes in inflammatory cytokines (Figure 1*A*–*C*). Lipocalin-2 (Lcn-2) is a secretory protein produced mainly by neutrophils and released in the feces after induction of colitis.[25] Therefore, Lcn-2 is considered a sensitive and noninvasive biomarker of intestinal inflammation. Analysis of Lcn-2 in stool samples collected from mice exposed to MDX (5%), PG (0.5%), and GEL (5 g/L) showed no significant change as compared with control mice, thus confirming the absence of colitis in mice fed such additives (Figure 1*D*). However, MDX-fed mice developed a more severe colitis when challenged with dextran sulfate sodium (DSS), as shown by significantly greater weight loss (Figure 2*A*), more pronounced infiltration of inflammatory cells, and greater epithelial damage (Figure 2*B* and *C*). The MDX-fed mice also showed up-regulation of interleukin (IL)1β and Lcn-2 as compared with mice receiving PG- or GEL-enriched diet or controls (Figure 2*D* and *E*). To ascertain at which concentration MDX exacerbated experimental colitis, we fed mice with MDX concentrations ranging from 1% to 5%. The deleterious effect of MDX on intestinal inflammation was more evident when it was used at a concentration of 5%, even though mice given 3% MDX showed a more pronounced inflammatory infiltrate as compared with mice receiving drinking water (Figure 2*F* and *G*). Therefore, all subsequent experiments were performed with 5% MDX.

To exclude that the more severe colitis in MDX-treated mice was owing to increased uptake of DSS, we used another model of intestinal inflammation induced by a single subcutaneous injection of indomethacin. MDX-fed mice showed a more pronounced ileal mucosal injury compared with controls (Figure 2*H* and *I*). Altogether, these data indicate that consumption of MDX in drinking water exacerbates gut inflammation.

Abbreviations used in this paper: **ATF, activating transcription factor; Chop, C/EBP homologous protein; DSS, dextran sodium sulfate; ER, endoplasmic reticulum; Ern-1, endoplasmic reticulum to nucleus signaling 1; GEL, animal gelatin; Grp78, glucose-regulated protein; HT29-MTX, _____; IBD, inflammatory bowel disease; IEC, intestinal epithelial cells; IL, interleukin; IRE, inositol-requiring enzyme; Lcn-2, lipocalin-2; LPMC, lamina propria mononuclear cells; MAPK, mitogen-activated protein kinase; MDX, maltodextrin; Muc-2, Mucin-2; OTU, _____; PBS, phosphate-buffered saline; PCR, polymerase chain reaction; PG, propylene glycol; p-p38, phosphorylated p38; siRNA, small interfering RNA; TUDCA, tauroursodeoxycholic acid; UPR, unfolded protein response.**

2352-345X
https://doi.org/10.1016/j.jcmgh.2018.09.002

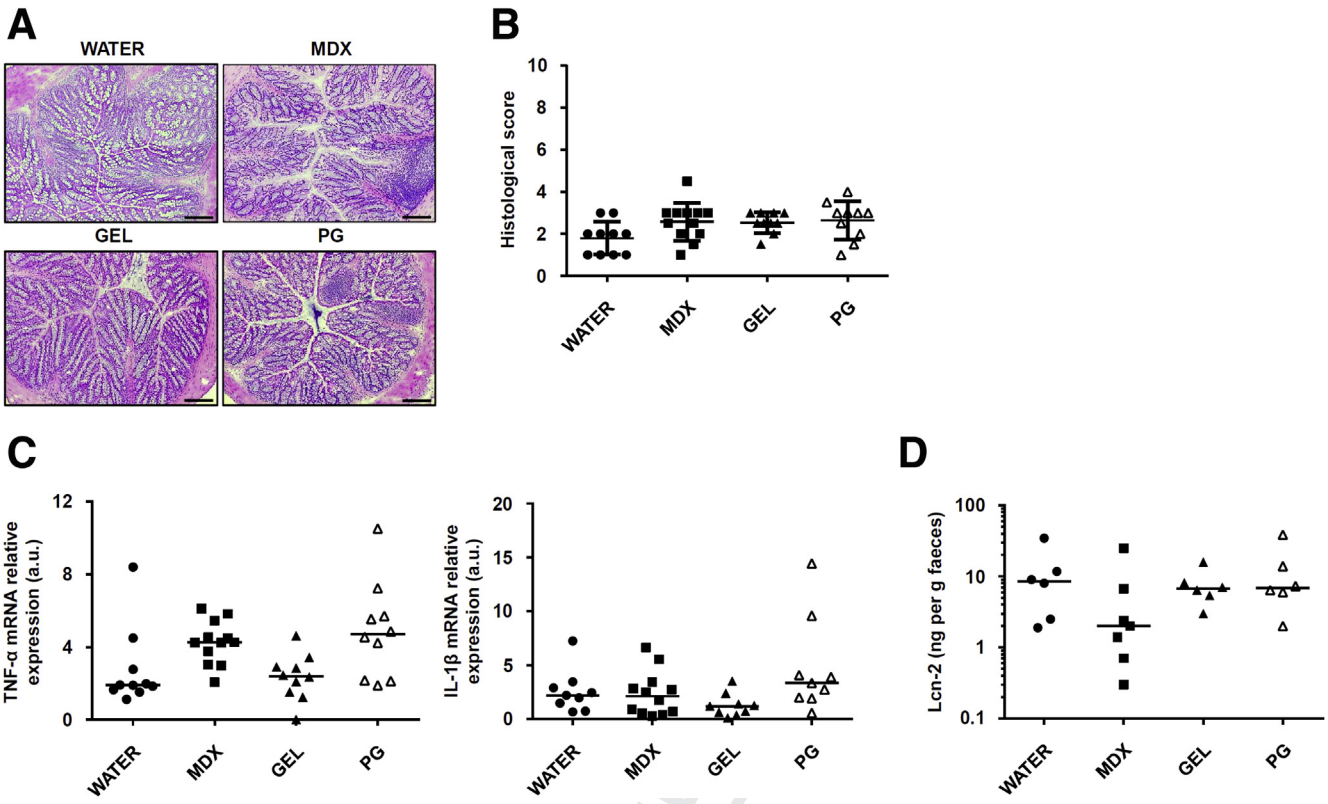

Figure 1. MDX, PG, and GEL do not induce intestinal inflammation. (*A*) Representative H&E staining of colon sections taken from wild-type mice exposed or not to 5% MDX, 0.5% PG, or 5 g/L GEL, all diluted in drinking water, for 45 days and then killed. The figure is representative of 9–12 mice/group from 3 independent experiments. *Scale bars*: 100 μm. (*B*) Histologic score of colonic tissues taken from mice fed as indicated in panel *A*. Data were generated using 9–12 mice/group from 3 independent experiments and expressed as means ± SD. Differences among groups were compared using 1-way analysis of variance followed by the Bonferroni post hoc test. (*C*) Expression of *Tnf-α* and *IL1β* RNA transcripts in colon tissues taken from mice fed as indicated in panel *A*. Data were generated using 9–12 mice/group from 3 independent experiments. Each *point* in the graph indicates the RNA expression of the specific transcript in the colon of a single mouse; *horizontal bars* indicate median value. Differences among groups were compared using the Kruskal–Wallis test. (*D*) Scatter plot showing levels of fecal Lcn-2 protein in mice fed as indicated in panel *A*. Data were generated using 6–7 mice/group from 3 independent experiments. *Horizontal bars* indicate median value. Differences among groups were compared using the Kruskal–Wallis test. mRNA, messenger RNA; TNF, tumor necrosis factor.

MDX Activates an Endoplasmic Reticulum Stress Response in Intestinal Epithelial Cells

To dissect the mechanisms by which MDX enhances susceptibility to intestinal damage, we performed a microarray analysis of colonic samples isolated from mice receiving MDX. Several genes involved in the lipid and carbohydrate metabolism and in protein glycosylation were up-regulated in MDX-treated mice (Figure 3*A*). Mice given MDX also showed increased transcripts of molecules involved in the unfolded protein response (UPR), usually activated upon accumulation of unfolded proteins in the endoplasmic reticulum (ER), a phenomenon termed *ER stress*. Activation of the UPR pathway promotes translational attenuation, refolding of unfolded proteins, and degradation of irreversibly unfolded proteins, with the downstream effect of restoring ER function. Among the UPR-related genes, *Ern-2*, which encodes for inositol-requiring enzyme (IRE)1β protein, was the most differentially expressed gene (Figure 3*A*). Real-time polymerase chain reaction (PCR) assay of colonic samples confirmed the microarray results and showed up-regulation of *Ern-1* and *Xbp1s*, 2 other IRE1/UPR-related genes (Figure 3*B*). In contrast, MDX caused no significant change in glucose-regulated protein (Grp78), activating transcription factor 6 (ATF6), ATF4, and C/EBP homologous protein (Chop) (Figure 3*C*), suggesting that MDX specifically induces IRE1-dependent signal transduction events. Further analysis of RNA transcripts in intestinal epithelial cells (IECs) and lamina propria mononuclear cells (LPMCs) isolated from colonic samples showed that induction of IRE1β/IRE1α was restricted to the intestinal epithelium compartment (Figure 3*D*). In vitro stimulation of intestinal crypts from untreated mice with MDX enhanced RNA transcripts for *Ern-1*, *Ern-2*, and *Xbp1s* (Figure 3*E*).

MDX-Enriched Diet Alters the Intestinal Mucus Barrier

IRE1β expression is restricted to the ER membrane of goblet cells in the small intestine and colon.[26] The major macromolecular component of the gut mucus layer is the

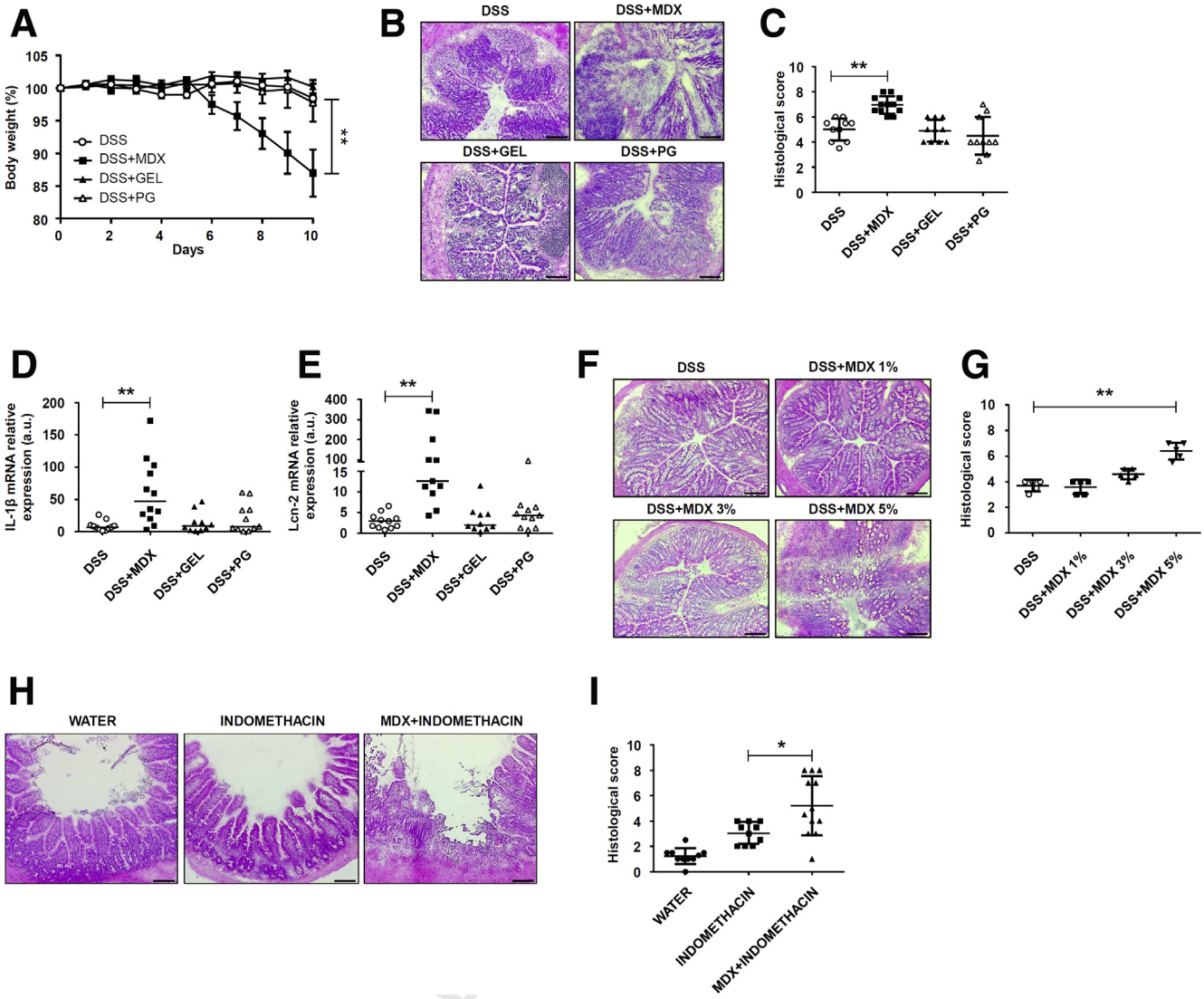

Figure 2. MDX-enriched diet exacerbates intestinal inflammation. (*A*) Wild-type mice were exposed to 5% MDX, 0.5% PG, or 5 g/L GEL, all diluted in drinking water, over a period of 45 days and challenged with DSS (1.75% in drinking water) starting from day 35 of diet. Body weight was recorded daily from day 35 until death (day 45). Data were generated using 10–12 mice per group from 3 independent experiments and expressed as means ± SEM. Differences among groups were compared using 1-way analysis of variance followed by the Bonferroni post hoc test. DSS vs DSS + MDX, $^{**}P \leq .01$. (*B* and *C*) Representative H&E staining and histologic score of colon sections taken from mice treated with DSS either alone or in combination with MDX, PG, or GEL, as indicated in panel *A*, and killed on day 45. Data were generated using 10–12 mice per group from 3 independent experiments and expressed as means ± SD. Differences among groups were compared using 1-way analysis of variance followed by the Bonferroni post hoc test. DSS vs DSS + MDX, $^{**}P \leq .01$. (*B*) *Scale bars*: 100 μm. (*D* and *E*) *IL1β* and *Lcn-2* RNA expression was assessed by real-time PCR in colonic tissues taken from mice treated as indicated in panel *A* and killed on day 45. Data were generated using 10–12 mice per group from 3 independent experiments. Each *point* in the graph indicates the RNA expression of the specific transcript in the colon of a single mouse; *horizontal bars* indicate median value. Differences among groups were compared using the Kruskal–Wallis test. DSS + MDX vs DSS, $^{**}P \leq .01$. (*F* and *G*) Representative H&E staining and histologic score of colon sections taken from mice treated with DSS either alone or in combination with increasing concentrations of MDX, as indicated in panel *A*, and killed on day 45. Data were generated using 5 mice per group from 2 independent experiments and expressed as means ± SD. Differences among groups were compared using 1-way analysis of variance followed by the Bonferroni post hoc test. 5% DSS + MDX vs DSS, $^{**}P \leq .01$. (*H* and *I*) Representative H&E staining and histologic score of ileum sections taken from wild-type mice exposed to 5% MDX diluted in drinking water for 35 days, and then treated with a single subcutaneous injection of indomethacin (5 mg/kg). Mice were killed 24 hours after indomethacin injection and tissues were collected for histopathologic analysis. Data were generated using 10–12 mice per group of 3 independent experiments and expressed as means ± SD. Differences among groups were compared using 1-way analysis of variance followed by the Bonferroni post hoc test ($^{*}P \leq .05$). *Scale bars*: 100 μm. mRNA, messenger RNA.

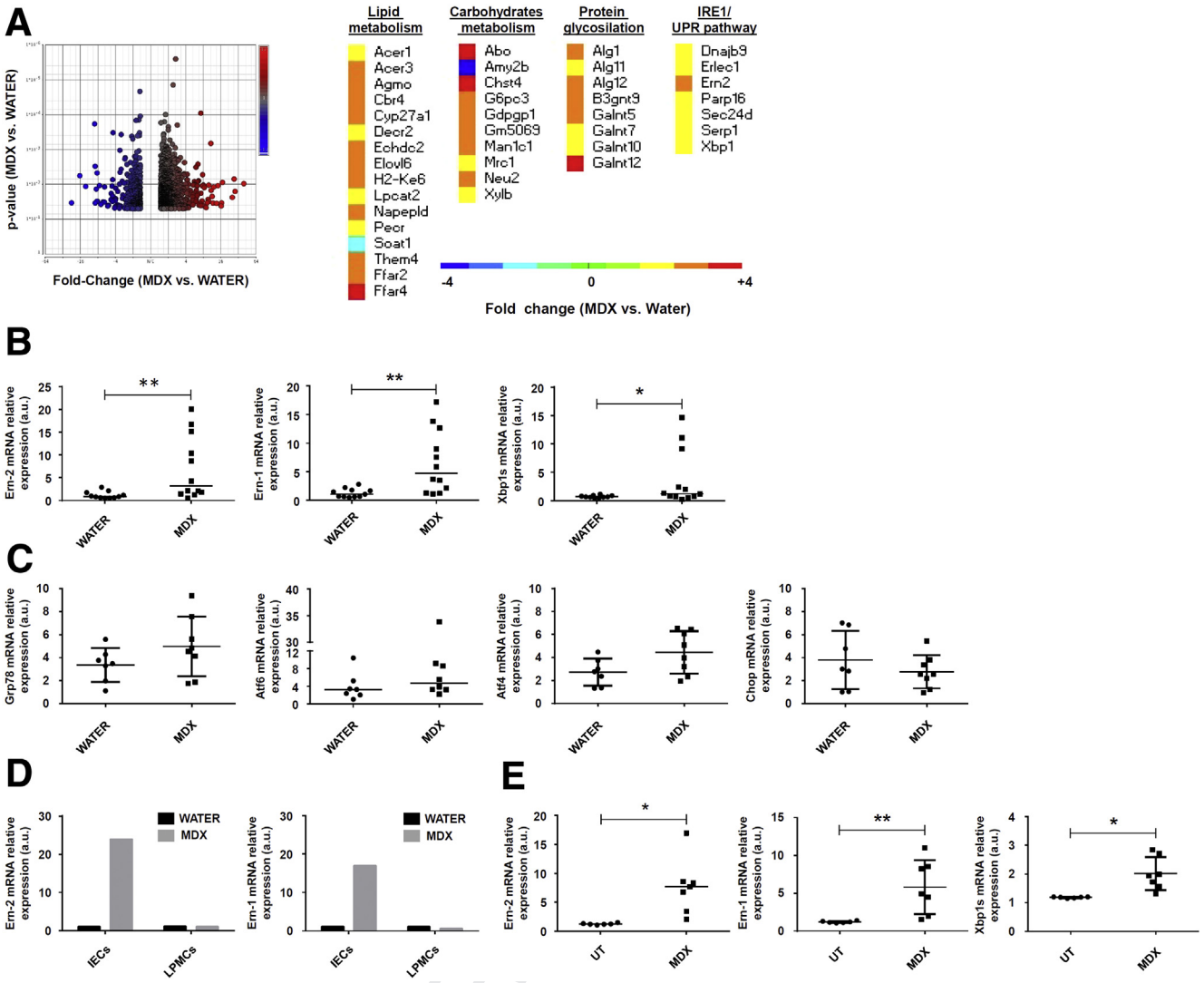

Figure 3. MDX up-regulates the IRE1-dependent UPR pathway in intestinal epithelial cells. (*A*) Volcano plot and heat map showing microarray-based differential expression, $\log_2$ (fold change) of genes related to lipid and carbohydrate metabolism, protein glycosylation, and UPR pathway of colon samples isolated from mice exposed to drinking water in the presence or absence of 5% MDX for 45 days without DSS. (*B*) *Ern-2*, *Ern-1*, and *Xbp1s* RNA expression was assessed by real-time PCR in total colonic samples. Data were generated using 11–12 mice per group from 3 independent experiments (*$P \leq .05$, **$P \leq .01$). Each *point* in the graph indicates the RNA expression of the specific transcript in the colon of a single mouse; *horizontal bars* indicate median value. Differences among groups were compared using the Mann–Whitney *U* test. (*C*) Scatter plots showing *Grp78*, *Atf6*, *Atf4*, and *Chop* RNA transcripts in colonic samples isolated from mice treated as indicated in panel *A*. Data were generated using 7–8 mice per group of 3 independent experiments. Each *point* in the graph indicates the RNA expression of the specific transcript in the colon of a single mouse; *horizontal bars* indicate median value or means ± SD. Differences among groups were compared using the Mann–Whitney *U* test or the 2-tailed Student *t* test. (*D*) Representative histograms showing *Ern-2* and *Ern-1* RNA expression in IECs and LPMCs isolated from a pool of 3–4 mice treated as indicated in panel *A*. The example is representative of 2 independent experiments in which similar results were obtained. (*E*) Scatter plots showing *Ern-2*, *Ern-1*, and *Xbp1s* RNA expression in intestinal crypts isolated from the colons of untreated mice and cultured in the presence or absence of MDX for 30 minutes. Data were generated using crypts isolated from 6–7 mice from 3 independent experiments (*$P \leq .05$, **$P \leq .01$). *Left*: *Horizontal bars* indicate median value and differences between groups were compared using 2-tailed Mann–Whitney *U* test. *Middle* and *right*: *Horizontal bars* indicate means ± SD and differences between groups were compared using the Student *t* test. mRNA, messenger RNA; UT, untreated.

mucin glycoprotein Mucin-2 (Muc-2), which contains cysteine-rich and highly glycosylated domains and requires extensive post-translational modification within the ER and Golgi.[27] The complexity of the mucin protein and the high secretory output of the goblet cells make Muc-2 prone to misfolding. Increased accumulation of Muc-2 precursors in the ER of goblet cells leads to a reduction of mucin secretion.[28] Immunofluorescence analysis of colonic sections showed that MDX markedly reduced Muc-2 staining, as well as expression of glycosylated (mature) Muc-2 (Figure 4*A*).

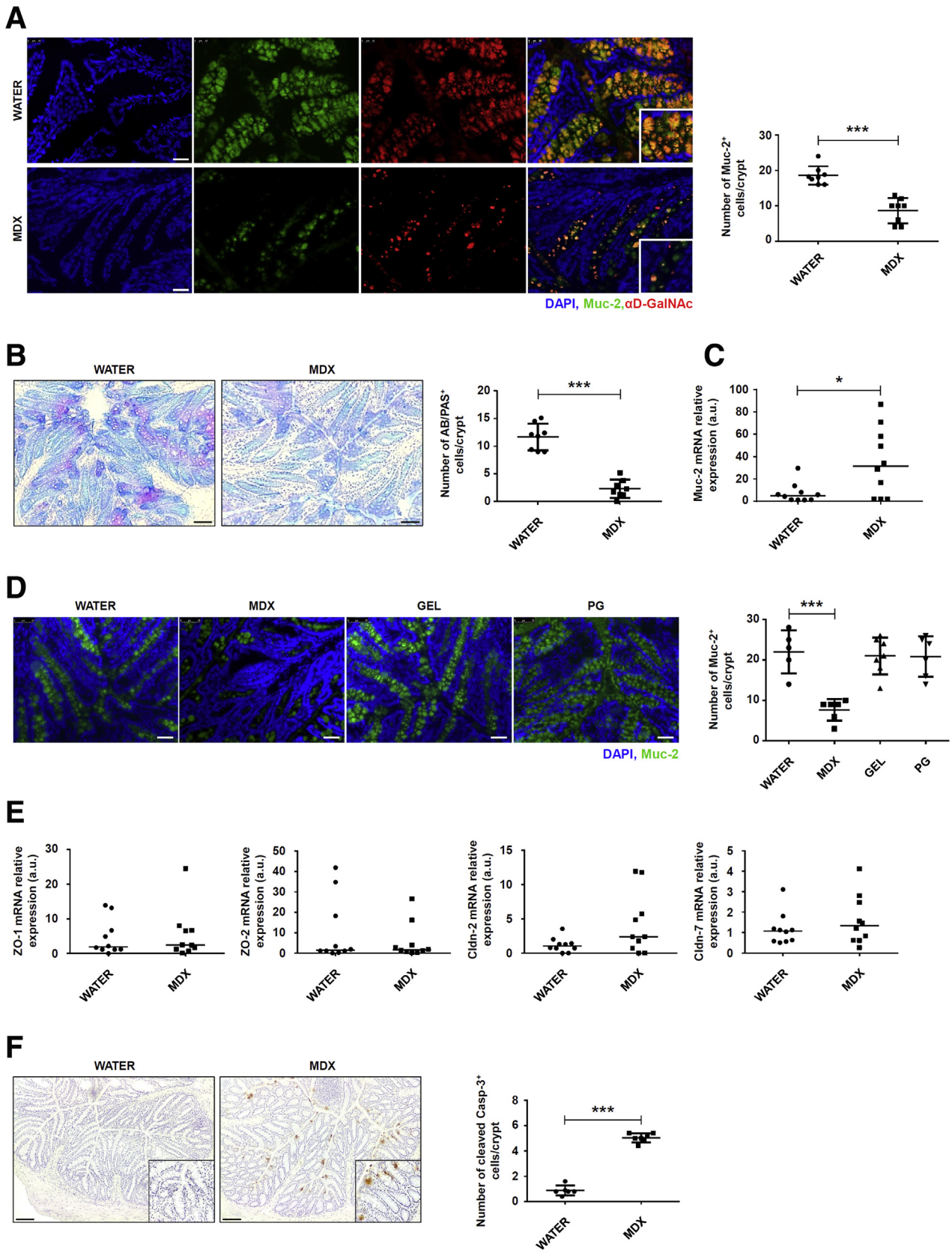
A
WATER
MDX
DAPI, Muc-2,αD-GalNAc
Number of Muc-2+ cells/crypt
***
WATER
MDX
B
WATER
MDX
Number of AB/PAS+ cells/crypt
***
C
Muc-2 mRNA relative expression (a.u.)
*
D
WATER
MDX
GEL
PG
DAPI, Muc-2
Number of Muc-2+ cells/crypt
***
E
ZO-1 mRNA relative expression (a.u.)
ZO-2 mRNA relative expression (a.u.)
Cldn-2 mRNA relative expression (a.u.)
Cldn-7 mRNA relative expression (a.u.)
F
WATER
MDX
Number of cleaved Casp-3+ cells/crypt
***

Moreover, periodic acid-Schiff/Alcian blue staining confirmed the negative effect of a MDX-enriched diet on mucus content (Figure 4*B*). In contrast, MDX up-regulated *Muc-2* RNA transcripts (Figure 4*C*), a finding that could reflect activation of a compensatory mechanism to the reduced Muc-2 protein secretion. Mice receiving PG or GEL showed no mucus depletion in the colon (Figure 4*D*). RNA transcripts for *zonulin-1*, *zonulin-2*, *claudin-2*, and *claudin-7* remained unchanged after MDX exposure (Figure 4*E*). Enhanced staining for cleaved caspase-3, indicative of induction of intestinal epithelial apoptosis, was seen in colonic sections of MDX-treated mice (Figure 4*F*).

Induction of ER Stress by MDX Is Mediated by p38 Mitogen-Activated Protein Kinase

We then examined the pathway(s) whereby MDX induces ER stress. Stimulation of the mucus-secreting HT29-MTX cell line with 3% and 5% MDX up-regulated *Ern-2* RNA transcripts (Figure 5*A*). To be consistent with the in vivo results, the subsequent in vitro studies were performed using 5% MDX. Increased concentrations of solutes, such as glucose, in the extracellular compartments were associated with augmented hypertonicity. Because hypertonic stress is sensed through the mitogen-activated protein kinase (MAPK) signaling pathway,[29,30] we investigated the involvement of such a pathway in the MDX-mediated IRE1β induction. Treatment of HT29-MTX cells with MDX caused a time-dependent increase in the expression of phosphorylated (p)-p38, while extracellular signal–regulated kinase 1/2 and c-Jun N-terminal kinase activation remained unchanged (Figure 5*B*). Pharmacologic inhibition of p38 down-regulated MDX-induced *Ern-2* RNA expression (Figure 5*C*). Similar results were seen in MDX-treated cells transfected with p38 small interfering RNA (siRNA) (Figure 5*D*). Immunofluorescence of mouse colonic sections showed that daily consumption of MDX enhanced p-p38 expression in epithelial cells (Figure 5*E*).

ER Stress Inhibition Improves Colitis in MDX-Fed Mice

To mechanistically prove that the enhanced susceptibility of mice to colitis after MDX administration relies on the ER stress/UPR pathway, we inhibited ER stress with the chemical chaperone tauroursodeoxycholic acid (TUDCA). First, we confirmed that TUDCA inhibited ER stress because pretreatment of HT29-MTX cells with TUDCA significantly reduced MDX-mediated *Ern-2* RNA expression (Figure 6*A*). Next, we showed that administration of TUDCA to MDX-treated mice resulted in diminished induction of *Ern-2*, *Ern-1*, and *Xbp1s* RNA expression and normalization of Muc-2 production (Figure 6*B* and *C*). In these experiments, TUDCA administration was started at day 21 because our data showed initial signs of ER stress at this time point after MDX administration (personal unpublished observations). Finally, we tested the modulatory effect of TUDCA on the course of DSS colitis. Mice receiving TUDCA showed a marked attenuation of DSS colitis after MDX administration, as evidenced by less changes in body weight, improved histology (Figure 6*D*–*F*), and lower *IL1β* and *Lcn-2* transcripts (Figure 6*G* and *H*).

Figure 4. (***See previous page***). **MDX-enriched diet alters intestinal mucous barrier.** (*A*) Immunofluorescence analysis of Muc-2 (green) and glycosylated (mature) Muc-2 (red) in colon sections isolated from mice exposed to drinking water in the presence or absence of 5% MDX for 35 days. Nuclei are stained with 4′,6-diamidino-2-phenylindole (DAPI) (blue). The figure is representative of 4 separate experiments. *Scale bars*: 25 μm. *Right*: Number of Muc-2–expressing cells per crypt. Data indicate means ± SD of the positive cells counted in 4 different fields per colon section and were generated using 8 mice per group from 4 independent experiments. Differences between groups were compared using the Student *t* test (***$P \leq .001$). (*B*) Periodic acid-Schiff (PAS)–Alcian blue (AB) staining of colonic sections taken from mice treated as indicated in panel *A*. The figure is representative of 3 separate experiments. *Right*: Number of Alcian blue/periodic acid-Schiff–expressing cells per crypt. Data indicate means ± SD of the positive cells counted in 4 different fields per colon section and were generated using 8 mice per group from 3 independent experiments. Differences between groups were compared using the 2-tailed Student *t* test (***$P \leq .001$). *Scale bars*: 10 μm. (*C*) Scatter plot showing *Muc-2* RNA expression in colon tissues taken from mice exposed to drinking water in the presence or absence of 5% MDX for 35 days. Data were generated using 10 mice per group from 3 independent experiments. Each *point* in the graph indicates the RNA expression of the specific transcript in the colon of a single mouse; *horizontal bars* indicate median value. Differences between groups were compared using the Mann–Whitney *U* test (*$P \leq .05$). (*D*) Immunofluorescence analysis of Muc-2 (green) in colon sections isolated from mice exposed to drinking water in the presence or absence of 5% MDX, 0.5 g/L GEL, or 0.5% PG for 35 days. Nuclei are stained with DAPI (blue). The figure is representative of 3 separate experiments. *Scale bars*: 50 μm. *Right*: Number of Muc-2–expressing cells per crypt. Data indicate means ± SD of the positive cells counted in 4 different fields per colon section and were generated using 5–7 mice per group from 3 independent experiments. Differences between groups were compared using the 2-tailed Student *t* test (***$P \leq .001$). (*E*) Scatter plot showing *zonulin-1*, *zonulin-2*, *claudin-2*, and *claudin-7* RNA expression in colon tissues taken from mice treated as indicated in panel *A*. Data were generated using 10 mice per group from 3 independent experiments. Each *point* in the graph indicates the RNA expression of the specific transcript in the colon of a single mouse; *horizontal bars* indicate median value. Differences between groups were compared using the Mann–Whitney *U* test (*$P \leq .05$). (*F*) Cleaved caspase-3–positive cells were evaluated in colon sections of mice treated as indicated in panel *A*. The figure is representative of 3 separate experiments. *Scale bars*: 100 μm. *Right*: Number of cleaved caspase-3–positive cells per crypt. Data indicate means ± SD of the positive cells counted in 4 different fields per colon section and were generated using 6–7 mice per group from 3 independent experiments. Differences between groups were compared using the Student *t* test (***$P \leq .001$). Cldn, claudin; mRNA, messenger RNA; ZO, zonula occludens.

MDX-Enriched Diet Does Not Affect Mucosa-Associated Microbiota

Interrogation of microbiota composition with 16S RNA sequencing in colonic samples showed that MDX-fed mice did not show any changes in microbiota composition in terms of phyla and related classes (Figure 7*A* and *B*), with low frequency (<0.1%) of the genus *E coli* among groups. TUDCA treatment was associated with no change in microbiota composition (Figure 7*A* and *B*).

Prolonged MDX-Enriched Diet Induces Low-Grade Intestinal Inflammation

Studies in mucin-deficient mice indicated that persistent mucus reduction can lead to the development of intestinal pathology.[28,31–33] Therefore, we assessed whether prolonged a MDX-enriched diet could favor the initiation of intestinal inflammation. Mice fed with MDX for 10 weeks showed no significant change in body weight and stool consistency (Figure 8*A* and *B*). However, such animals showed low-grade intestinal inflammation, which was characterized by focal inflammatory infiltrates, distortion of gland architecture, edema, and increased transcripts for *IL1β*, *Lcn-2*, and *Ern-2* as compared with control mice (Figure 8*C–E*). As expected, mice receiving MDX had a marked reduction of Muc-2 protein (Figure 8*F*).

Because recent studies reported that low-grade inflammation induced by food additives was associated with metabolic alterations,[19,22] we investigated whether a prolonged MDX-enriched diet could alter blood glycemic levels. Data shown in Figure 8*G* indicate that the 15-hour fasting blood glucose level was higher in MDX-treated mice as compared with controls (Figure 8*G*).

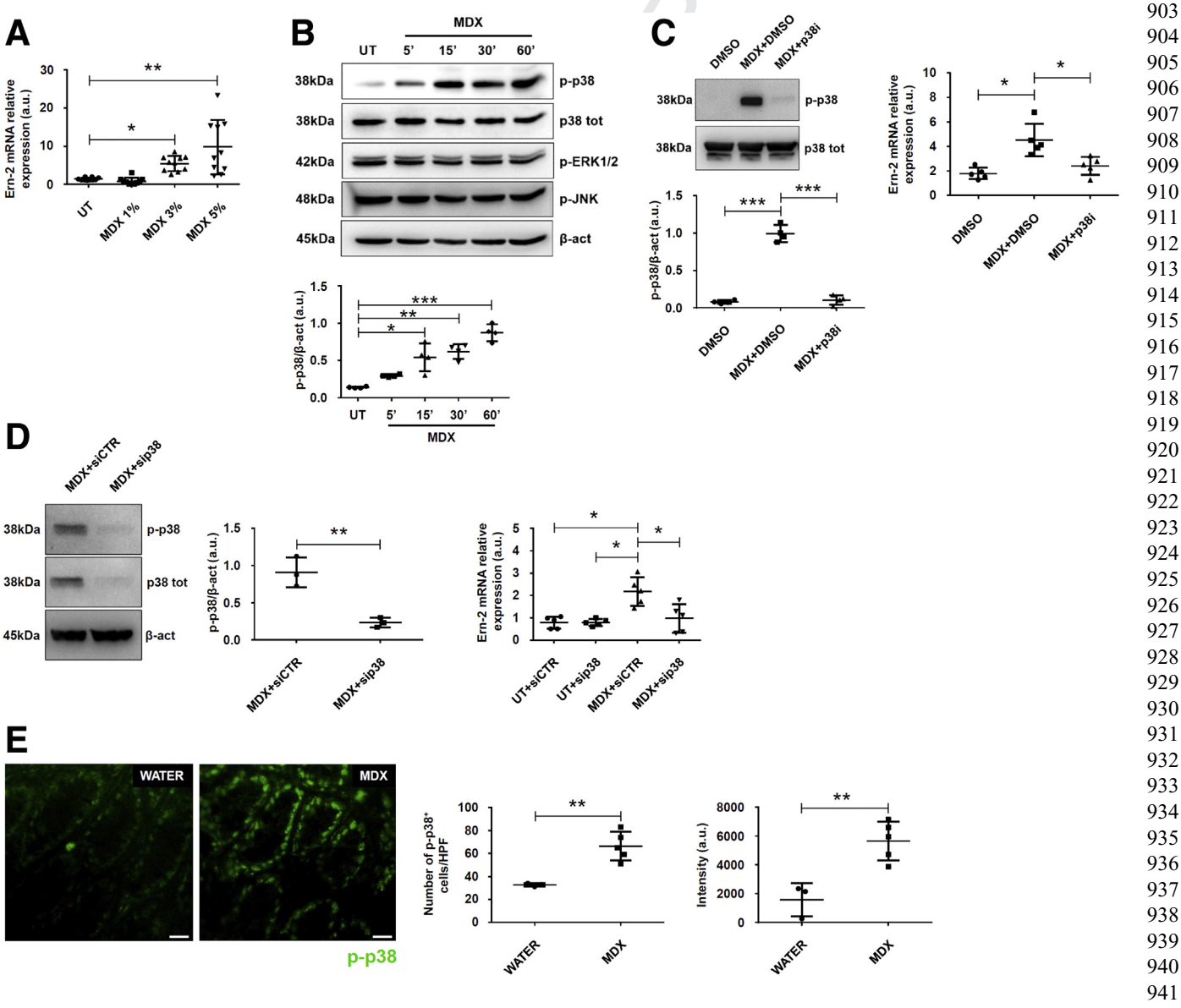

Discussion

This study was performed to ascertain whether food additives commonly used in the Western diet could promote/exacerbate gut inflammation. Initial experiments showed that daily consumption of each of 3 common food additives, namely MDX, PG, and GEL for 45 days, did not induce overt colitis. However, mice given MDX, but not PG or GEL, showed increased severity of intestinal inflammation after DSS or indomethacin administration. The concentration of MDX selected for this study (ie, 5%) is equivalent to levels commonly found in infant formulas,[24] even though it is highly likely that the amount of MDX reaching the distal intestine is lower than what was administered to mice. We next performed a microarray analysis of colon samples from MDX-treated mice to determine the mechanisms involved. Among the most upregulated genes in the MDX-treated mice was *Ern-2*, which encodes for IRE1β, a sensor of ER stress that mitigates the uncontrolled activation of ER stress response in epithelial cells. Indeed, IRE1β is expressed in intestinal epithelial and airway mucus cells, where it promotes efficient protein folding and secretion of mucins by regulating the level of Muc-2 RNA.[26,34] Therefore, it is plausible that IRE1β upregulation in the colons of MDX-fed mice reflects the activation of a counter-regulatory mechanism that attempts to limit ER stress response in goblet cells. Next, we evaluated whether MDX altered the production of mucus. Mice receiving MDX had marked reduction of O-linked, glycosylated, mature Muc-2, even though they showed increased Muc-2 RNA expression. Altogether, these results indicate that mucus depletion seen in MDX-fed mice reflects alterations in Muc-2 maturation/folding and secretion rather than being a consequence of a defect in goblet cell development. In line with the earlier-described findings, in vitro stimulation of murine intestinal crypts and mucus-secreting HT29-MTX cells with MDX increased IRE1β expression.

Our data suggest a model in which MDX-enriched diet triggers the ER stress sensor IRE1β in intestinal epithelial cells via p38 MAPK, because MDX increased the expression of p-p38 in mice and HT29-MTX cells. Moreover, pharmacologic inhibition of p38 with SB202190, which is known to interfere with p38 MAP kinase activity[35] and to partially impair p38 phosphorylation through an indirect or feedback response mechanism,[36–38] or silencing of p38 with siRNA- Q15 abrogated MDX-driven IRE1β expression. The effect of MDX on Muc-2 content appears to be specific because MDX did not affect expression of other epithelial proteins (ie, defensins, zonulins, and claudins).

We surmise that induction of ER stress in goblet cells is functionally relevant to the detrimental effects of MDX because pretreatment of mice with TUDCA, a chemical chaperone that inhibits ER stress, prevented MDX-mediated *Ern-2* RNA overexpression and Muc-2 protein downregulation, as well as the detrimental effect of MDX on DSS-induced colitis. Because TUDCA was reported to exert other protective functions in the gut (eg, reduction of proinflammatory cytokine synthesis and improvement of intestinal barrier function),[39,40] we cannot exclude the possibility that TUDCA-mediated prevention of intestinal damage in colitic mice receiving MDX can in part rely on other potential regulatory effects of the compound.

Our data support previous studies showing that goblet cells are one of the major cells that tend to undergo ER stress in the intestinal epithelium.[28,41] This diminishes the

Figure 5. (***See previous page***). **MDX induces IRE1β expression via P38 MAPK.** (*A*) MDX induces *Ern-2* expression in the HT29-MTX cell line. Cells were either left untreated (UT) or cultured with increasing concentrations of MDX for 1 hour. *Ern-2* RNA transcripts were assessed by real-time PCR. Data are means ± SD of 10 samples per group derived from 4 independent experiments. Differences among groups were compared using 1-way analysis of variance followed by the Bonferroni post hoc test (**$P \leq .01$, *$P \leq .05$). (*B*) HT29-MTX cells were either left UT or stimulated with 5% MDX for the indicated time points. p-p38, p38, phosphorylated extracellular signal–regulated kinase 1/2 (p-ERK1/2), phosphorylated c-Jun N-terminal kinase Q36 (p-JNK), and β-actin (β-act) expression were analyzed by Western blot. One of 4 representative experiments in which similar results were obtained is shown together with densitometry analysis (*lower panel*). Data are means ± SD. Differences among groups were compared using 1-way analysis of variance followed by the Bonferroni post hoc test (*$P \leq .05$, **$P \leq .01$, ***$P \leq .001$). (*C*) Effect of the p38 inhibitor (p38i) on MDX-mediated p38 activation. HT29-MTX cells were stimulated or not with MDX for 1 hour in the presence or absence of p38i (10 μmol/L) or dimethyl sulfoxide (DMSO) (vehicle). p-p38 and p38 expression was assessed by Western blot. One of 4 representative experiments in which similar results were obtained is shown together with the densitometry analysis (*lower panel*). Data are means ± SD. Differences among groups were compared using 1-way analysis of variance followed by the Bonferroni post hoc test (***$P \leq .001$). *Right*: Effect of p38i on MDX-mediated *Ern-2* upregulation. HT29-MTX cells were stimulated or not with MDX for 1 hour in the presence or absence of p38i (10 μmol/L) or DMSO (vehicle) and *Ern-2* RNA transcripts evaluated by real-time PCR. Data are means ± SD of 5 independent experiments. Differences among groups were compared using 1-way analysis of variance followed by the Bonferroni post hoc test (*$P \leq .05$). (*D*) Effect of p38 knock-down on MDX-mediated *Ern-2* up-regulation. HT29-MTX cells were transfected with either control or p38 siRNA (CTR or p38 siRNA, respectively) for 18 hours and then stimulated or not with 5% MDX for 1 hour. Representative Q37 Western blot for p-p38, p38, and β-actin expression are shown in the *left panels* together with the densitometry analysis. Data are means ± SD of 3 independent experiments. Differences between groups were compared using the 2-tailed Student *t* test (**$P \leq .001$). *Right*: Expression of *Ern-2* RNA transcripts assessed by real-time PCR. Data are means ± SD of 5 independent experiments. Differences among groups were compared using 1-way analysis of variance followed by the Bonferroni post hoc test (*$P \leq .05$). (*E*) Immunofluorescence analysis of p-p38 (green) in colon samples isolated from MDX-fed mice and controls killed on day 45. The figure is representative of 3 separate experiments in which similar results were obtained. *Right panels* show the number and intensity of p-p38–expressing cells per field of colon section. Data are expressed as means ± SD and were generated using 3–5 mice per group from 3 independent experiments. Differences between groups were compared using the 2-tailed Student *t* test (**$P \leq .01$). mRNA, messenger RNA.

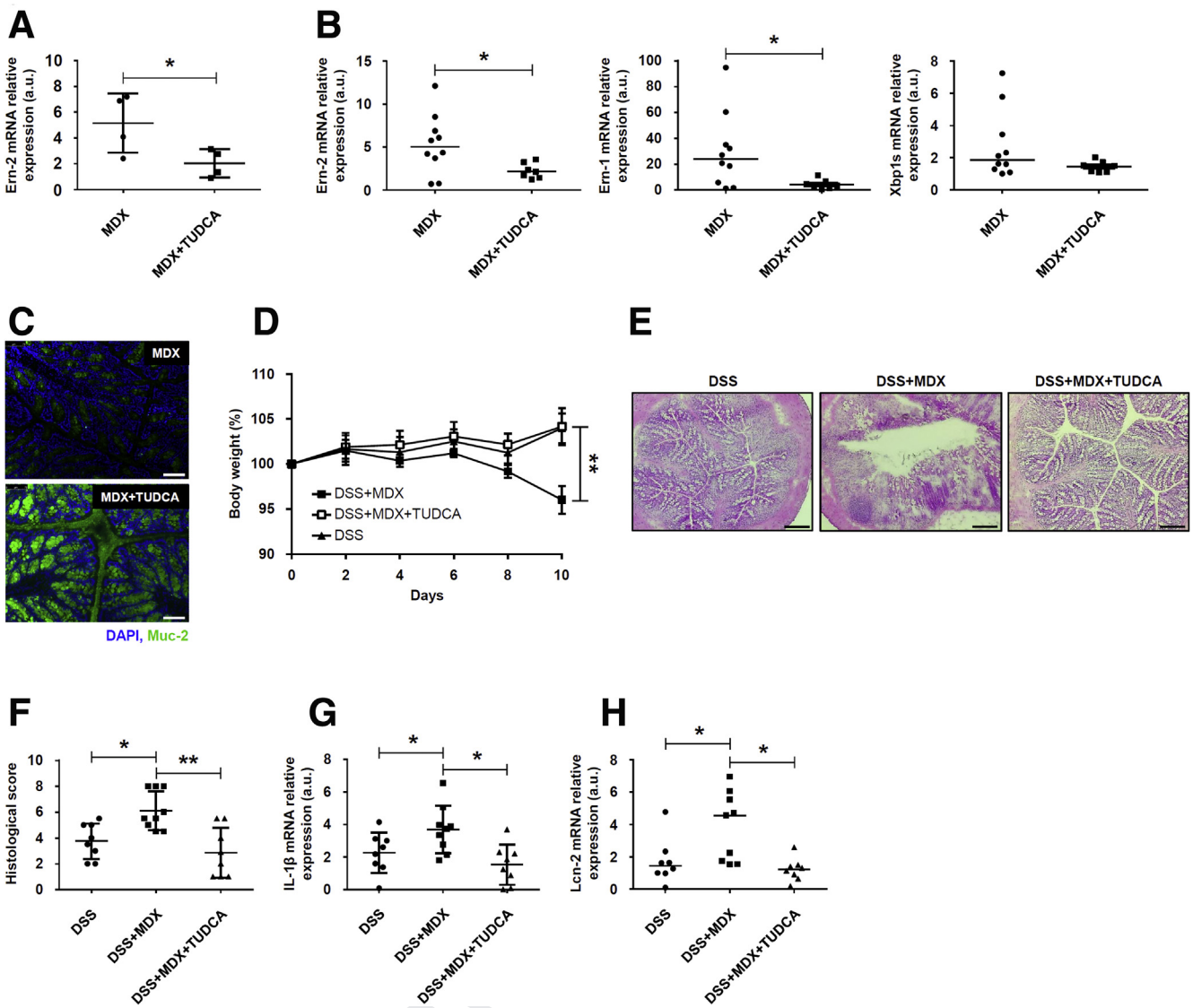

Figure 6. ER stress inhibition reduces MDX-mediated Ern-2 up-regulation and improves colitis in MDX-fed mice. (*A*) HT29-MTX cells were pretreated with TUDCA (10 μmol/L) or dimethyl sulfoxide (vehicle) and then stimulated with MDX for 1 hour. *Ern-2* RNA transcripts were analyzed by real-time PCR. Data are means ± SD of 4 independent experiments. Differences between groups were compared using the 2-tailed Student *t* test (*$P \leq .05$). (*B* and *C*) Wild-type mice were exposed to drinking water supplemented with 5% MDX for 45 days and injected or not with TUDCA (250 mg/kg intraperitoneally) every other day starting from day 21. Mice were killed on day 45, colonic tissues were isolated, and (*B*) *Ern-2*, *Ern-1*, and *Xbp1s* RNA transcripts and (*C*) *Muc-2* protein expression were evaluated by real-time PCR and immunofluorescence, respectively. (*B*) Data were generated using 7–10 mice per group from 3 independent experiments. Each *point* in the graph indicates the RNA expression of the specific transcript in the colon of a single mouse; *horizontal bars* indicate median value. Differences between groups were compared using the Mann–Whitney *U* test (*$P \leq .05$). (*C*) Pictures are representative of 4 separate experiments in which similar results were obtained. *Scale bars*: 25 μm. (*D*) Wild-type mice were exposed to drinking water supplemented with 5% MDX for 45 days and injected or not with TUDCA (250 mg/kg intraperitoneally) every other day starting from day 21. Mice were exposed to 1.75% DSS to induce colitis starting from day 35 until death (day 45), and body weight was recorded every other day. Data were generated using 8–9 mice per group from 3 independent experiments and expressed as means ± SEM. Differences among groups were compared using 1-way analysis of variance followed by the Bonferroni post hoc test (**$P \leq .01$). (*E* and *F*) Representative H&E staining of colon sections of mice treated as indicated in panel *D* and killed on day 45. (*F*) Scatter plot shows the histologic score. Data were generated using 8–9 mice per group from 3 independent experiments and expressed as means ± SD. Differences among groups were compared using 1-way analysis of variance followed by the Bonferroni post hoc test (*$P \leq .05$; **$P \leq .01$). (*G* and *H*) Representative scatter plots showing (*G*) *IL1β* and (*H*) *Lcn-2* RNA expression in colon tissues taken from mice treated as indicated in panel *D* and killed on day 45. Each *point* in the graph indicates the RNA expression of the specific transcript in the colon of a single mouse; *horizontal bars* indicate median value or means ± SD. Data were generated using 8–9 mice per group from 3 independent experiments. Differences among groups were compared using the Kruskal–Wallis test or 1-way analysis of variance followed by the Bonferroni post hoc test (*$P \leq .05$). DAPI, 4′,6-diamidino-2-phenylindole; mRNA, messenger RNA.

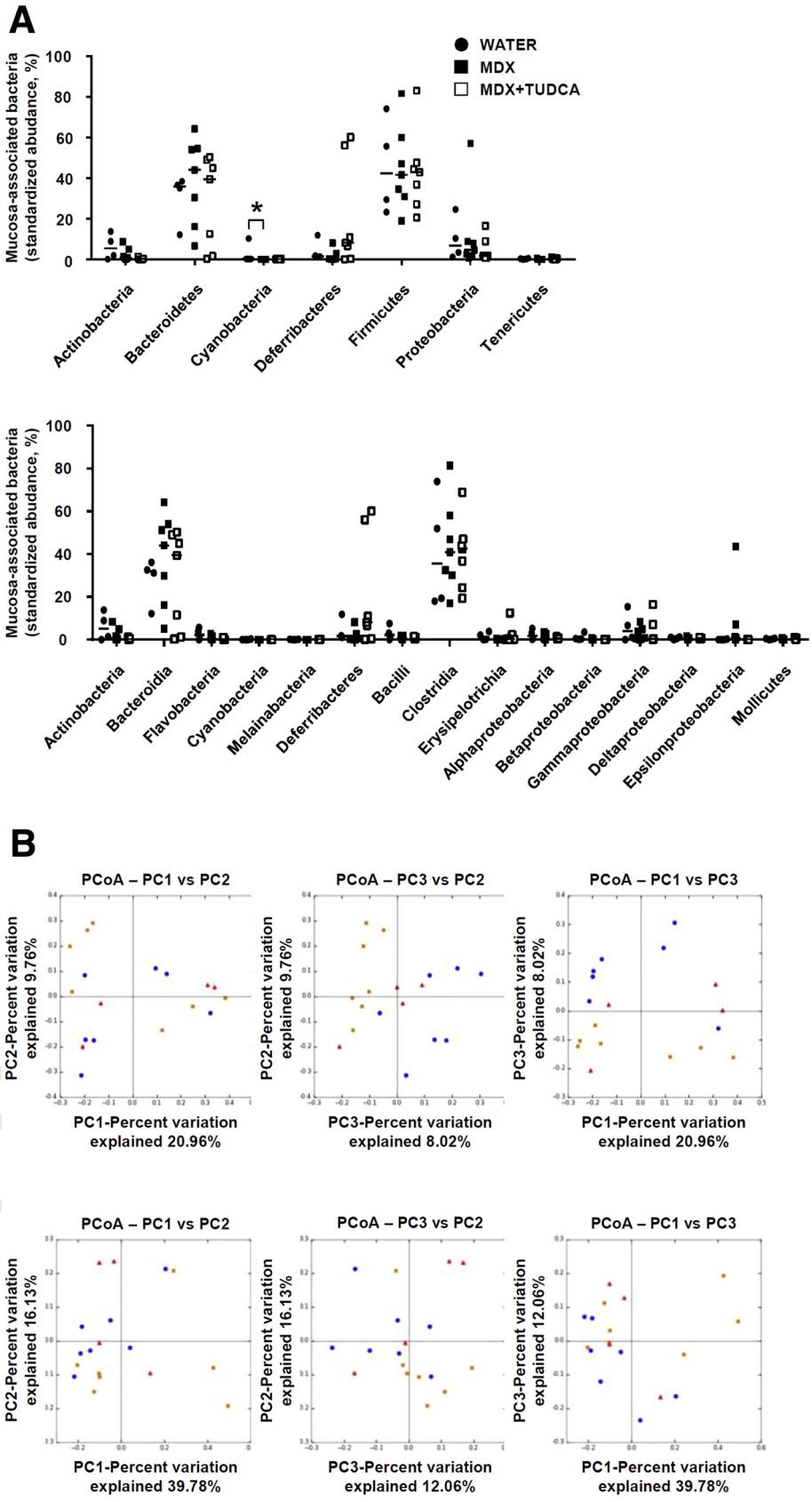

Figure 7. Effect of MDX on mucosa-associated microbiota. (*A* and *B*) Wild-type mice were exposed to drinking water supplemented with 5% MDX for 45 days and injected or not with TUDCA (250 mg/kg intraperitoneally) every other day starting from day 21. Control mice received drinking water for 45 days. All mice were killed on day 45. (*A*) Relative abundance of phyla and classes are represented for colonic mucosa-associated microbiota. *Horizontal bars* indicate median value. Data were generated using 4–7 mice per group from 2 independent experiments. Differences among groups were compared using the Kruskal–Wallis test (*$P \leq .05$). (*B*) Principal coordinates analysis (PCoA) of the unweighted and weighted UniFrac distance matrix of mucosa-associated bacteria from mice treated as indicated in panel *A*.

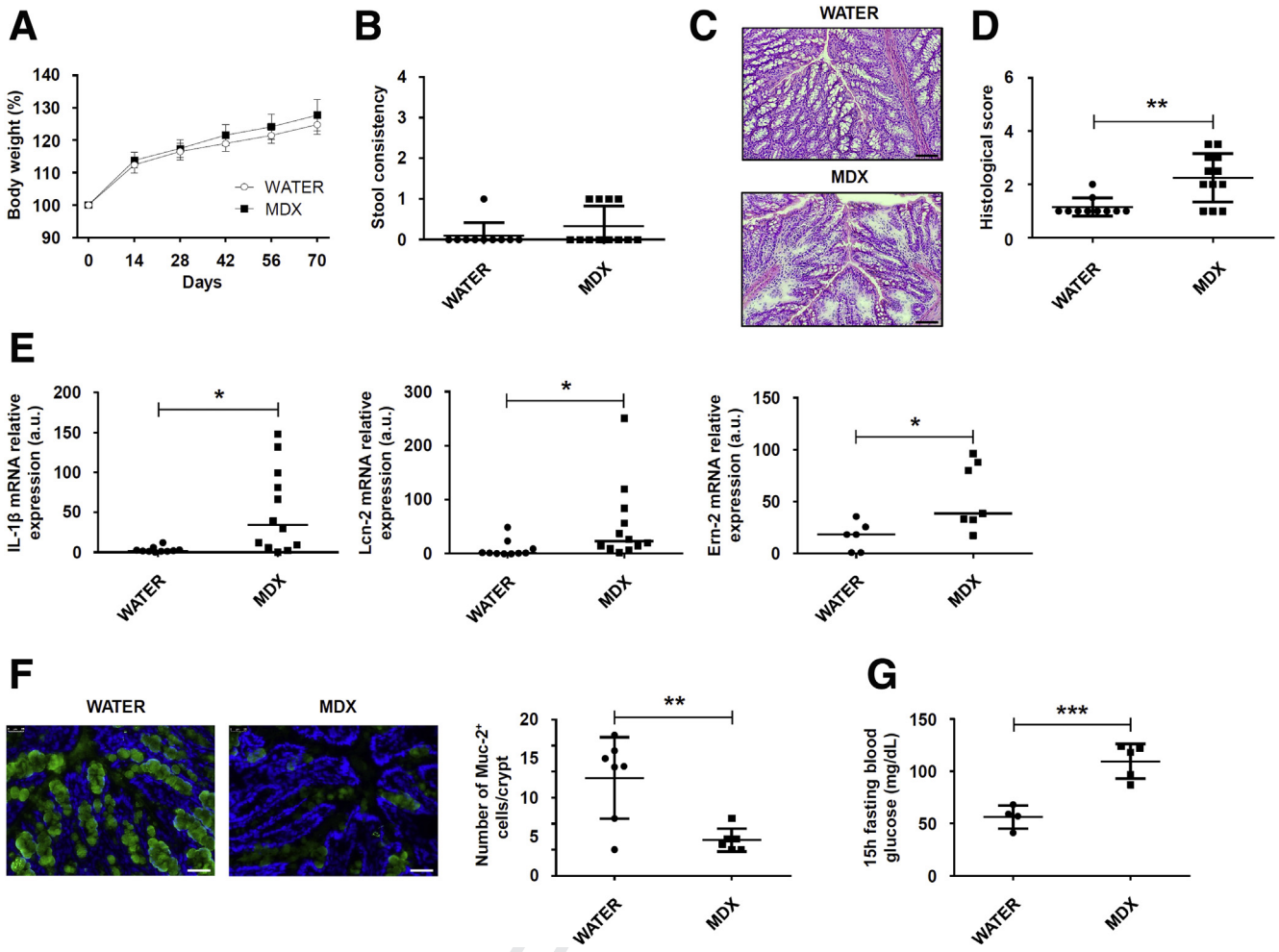

Figure 8. Prolonged MDX-enriched diet induces low-grade intestinal inflammation. Wild-type mice were exposed to 5% MDX diluted in drinking water for 10 weeks. (*A*) Body weight was recorded every 2 weeks until death (day 70). Data were generated using 10–12 mice per group from 3 independent experiments and are expressed as means ± SEM. Differences between groups were compared using the 2-tailed Student *t* test. (*B*) Scatter plots showing stool consistency of mice receiving 5% MDX diluted in drinking water for 10 weeks. Data were generated using 10–12 mice per group of 3 independent experiments and expressed as means ± SD. Differences between groups were compared using the 2-tailed Student *t* test. (*C* and *D*) Representative H&E staining of colon sections and histologic score of wild-type mice exposed to drinking water supplemented or not with 5% MDX for 10 weeks. *Scale bars*: 100 μm. Data were generated using 10–12 mice per group from 3 independent experiments and expressed as means ± SD. Differences between groups were compared using the 2-tailed Student *t* test (**$P \leq .01$). (*E*) Expression of *IL1β*, *Lcn-2*, and *Ern2* RNA transcripts in colon tissues taken from mice fed as indicated in panel *A*. Data were generated using 6–12 mice per group from 3 independent experiments. Each *point* in the graph indicates the RNA expression of the specific transcript in the colon of a single mouse; *horizontal bars* indicate median value. Differences between groups were compared using the Mann–Whitney *U* test (*$P \leq .05$). (*F*) Immunofluorescence analysis of Muc-2 (green) in colon samples isolated from mice fed with or without MDX for 10 weeks. *Scale bars*: 25 μm. The figure is representative of 3 separate experiments in which similar results were obtained. *Right panel* shows the number of Muc-2–expressing cells per crypt. Data indicate means ± SD of the positive cells counted in 4 different fields per colon section and were generated using 6–7 mice per group from 3 independent experiments. Differences between groups were compared using the 2-tailed Student *t* test (**$P \leq .01$). (*G*) Fifteen-hour–fasting blood glucose level in mice fed as indicated in panel *A*. Data were generated using 4–5 mice per group from 2 independent experiments and expressed as means ± SD. Differences between groups were compared using the 2-tailed Student *t* test (***$P \leq .001$). mRNA, messenger RNA.

integrity of the mucus barrier by reducing biosynthesis and mucin secretion.[28] The ability of MDX to promote ER stress appears unique because other food additives, such as titanium dioxide, have been reported to damage intestinal epithelial cells through a mechanism mediated by oxidative stress and independent of ER stress.[42] After synthesis by goblet cells, Muc-2 is secreted into the lumen and forms a protective mucus gel layer that acts as a selective barrier to protect the epithelium from mechanical stress, noxious agents, bacteria, and other pathogens.[43–45] Indeed, in the absence of a mucus layer, as in Muc-2–deficient mice, colonization of enteric pathogens occurs to a greater extent and more readily than in wild-type animals.[46] Moreover, after infection with specific pathogens (eg, *Citrobacter*

rodentium, *Entamoeba histolytica*), Muc-2–deficient mice show greater damage to the epithelium and have more colonic ulceration.[47,48]

Mucosa-associated microbiota composition remained unchanged on a MDX-enriched diet, arguing against the hypothesis that mucosal dysbiosis plays a key role in the negative effect of MDX on mucus formation. Our results differ from recently published data showing that dietary emulsifiers promote modest disturbances of the luminal microbiota, thus resulting in low-grade inflammation in wild-type mice, inducing severe alterations of gut microbiota composition, promoting robust colitis in mice lacking the immune-regulatory cytokine IL10, and negatively impacting the luminal microbiota composition in human beings.[19,49] Overall, the earlier-described observations indicate that multiple dietary components can alter intestinal homeostasis, contributing to the initiation and progression of pathologic conditions. In this context, it has been proposed that changes in the mucus barrier or biosynthesis of mucins play a role in the onset and persistence of IBD. In particular, in the inflamed colons of patients with ulcerative colitis, the mucus layer is thin owing to decreased Muc-2 production and secretion resulting from goblet cell depletion.[46] Indeed, these cells contain fewer mucin granules, which are filled with a nonglycosylated Muc-2 precursor, a finding that resembles that seen in mice exposed to MDX. Similarly, there is evidence that alterations in the amount and composition of the mucus barrier lead to IBD-like pathology in mice and that decreased Muc-2 output resulting from ER stress can diminish the mucus barrier and ultimately trigger inflammation.[28] This hypothesis is supported further by our demonstration that persistent mucus depletion in mice receiving a long-term MDX diet leads to low-grade inflammation.

In conclusion, this study shows that a MDX-enriched diet reduces the intestinal content of Muc-2, thus making the host more sensitive to colitogenic stimuli. These data together with the demonstration that MDX can promote epithelial intestinal adhesion of pathogenic bacteria[21] supports the hypothesis that Western diets rich in MDX can contribute to gut disease susceptibility.

Materials and Methods

Mice

Balb/c mice (age, 6–7 wk) were purchased from Charles River Laboratories Italia Srl and hosted in the animal facility at the University of Rome Tor Vergata (Rome, Italy). All in vivo experiments were approved by the animal ethics committee according to Italian legislation on animal experimentation.

Food Additive Treatment and Experimental Gut Inflammation

MDX (dextrose equivalent, 4.0–7.0; #419672) and propylene glycol (>99.5% FCC; #W294004) were purchased from Sigma (Milan, Italy). Animal gelatin from bovine and porcine bones was purchased from Honeywell Fluka (Milan, Italy) (#53028). Mice were exposed to MDX (concentration range, 1%–5%), PG (0.5%), and GEL (5 g/L) in drinking water for 45 days. Water was changed every second day. During the last 10 days, animals received DSS (1.75%, #160110; MP Biomedicals, Santa Ana, CA) either in normal drinking water, or MDX-, PG-, or GEL-enriched drinking water. Mice were weighed daily. Mice were killed after 10 days of treatment with DSS and colon samples were collected for histology, protein and RNA extraction, and isolation of IECs and LPMCs. In parallel, mice receiving a MDX-enriched diet, together with control mice, were given 250 mg/kg TUDCA (Carbosynth Ltd, Berkshire, UK) intraperitoneally every other day starting from day 21 of diet.

In additional experiments, mice were exposed to drinking water in the presence or absence of MDX 5% for 35 days and then injected subcutaneously with indomethacin (5 mg/kg, #I7378; Sigma). Mice were killed 24 hours later and ileal samples were collected for histologic analysis.

Cell Isolation and Cultures

IECs and LPMCs were isolated from murine colons as described previously.[50] Cells were resuspended in lysis buffer supplemented with 1% β-mercaptoethanol and stored at -80°C until RNA extraction. To isolate murine crypts, fresh colon specimens were cut in 5-mm size fragments and incubated in Dulbecco's modified Eagle medium containing 15 mmol/L EDTA for 1 hour at 4°C. The resulting crypts were stimulated with MDX 5% for 30 minutes and then resuspended in lysis buffer supplemented with 5% β-mercaptoethanol and stored at -80°C until RNA extraction.

The mucous-secreting HT29-MTX cell line was obtained from the European Collection of Authenticated Cell Cultures (Public Health England, Porton Down, Salisbury, UK). Cells were cultured in Dulbecco's modified Eagle medium supplemented with 10% fetal bovine serum, penicillin (0.1%), and streptomycin (0.1%). Subconfluent cells were cultured in the presence of increasing concentrations of MDX (from 1% to 5%) for 1 hour or with MDX 5% for different time points (5 minutes, 15 minutes, 30 minutes, and 1 h). In some experiments, HT29-MTX cells were pretreated with TUDCA (10 μmol/L) or a p38-MAPK inhibitor (S202190; Calbiochem, San Diego, CA) for 1 hour or transfected with p38 or a control siRNA (Santa Cruz, Dallas, TX) using Lipofectamine 2000 reagent (Invitrogen, Carlsbad, CA). After stimulation with MDX, cells were collected and pellets were immediately stored at -80°C for protein extraction, or resuspended in lysis buffer supplemented with 1% β-mercaptoethanol and stored at -80°C until RNA extraction.

Transcriptome Analysis

Total RNA was extracted from colon samples using the PureLink Purification technology kit with the RNase-free DNase set (Thermo Fisher Scientific, Monza, Italy). Samples with quantified complementary DNA were sequenced in the Microarray Unit of the Consortium for Genomic Technologies (Milan, Italy) by hybridization to GeneChip Mouse Gene 2.0 ST microarrays. Signal intensities of fluorescent images produced during GeneChip hybridizations were read by an Affymetrix Model 3000 Scanner.

Transcripts were selected on base of fold change value of 2 or higher. All the transcripts present on the GeneChip array were mapped to related classes by Gene Onthology, which provided the fold change generated from the comparison between MDX vs WATER. All the lists were annotated using the latest version of Affymetrix GeneChip Mouse Gene ST 2.0 annotations provided by NetAffx portal. The microarray data set has been deposited in the Gene Expression Omnibus databank (accession no. GSE117639; https://www.ncbi.nlm.nih.gov/geo/query/acc.cgi?acc=GSE117639).

Real-Time PCR

Total RNA was isolated from colon biopsy specimens and cells using PureLink Purification technology (Thermo Fisher Scientific). A constant amount of RNA (1 μg/sample) was retrotranscribed into complementary DNA. Reverse-transcription was performed with Oligo(dT) primers and with M-MLV reverse-transcriptase (Thermo Fisher Scientific). Real-time PCR was performed for murine IL1β, Lcn-2, tumor necrosis factor-α, interferon-γ, IL17A, endoplasmic reticulum to nucleus signaling 1 (Ern-1), Ern-2, β-defensin-1, zonulin-1, claudin-7, spliced X-box binding protein 1, activating transcription factor 4, activating transcription factor 4, and Chop using the IQ SYBR Green Supermix (Bio-Rad Laboratories, Milan, Italy), and for murine zonulin-2, claudin-2, and human Ern-2 using TaqMan Gene Expression Assays (Thermo Fisher Scientific). RNA expression was calculated relative to the β-actin gene using the $\Delta\Delta$Ct algorithm.

Quantification of Fecal Lipocalin-2 by Enzyme-Linked Immunosorbent Assay

Fecal samples were weighted and resuspended in phosphate-buffered saline (PBS) containing 0.1% Tween 20 at a final concentration of 100 mg/mL. Samples then were vortexed for 20 minutes and centrifugated for 10 minutes at 14,000g and 4°C. Supernatants then were collected and stored at -80°C until analysis. Lcn-2 protein levels were quantified using the Duoset murine LCN-2 enzyme-linked immunosorbent assay kit (R&D Systems, Minneapolis, MN), and optical density was read at 450 nm.

Western Blot

Cells were lysed on ice in buffer containing 10 mmol/L HEPES (pH 7.9), 10 mmol/L potassium chloride, 0.1 mmol/L EDTA, 0.2 mmol/L ethylene glycol-bis (β-aminoethyl ether)-N,N,N′,N′-tetraacetic acid, and 0.5% Nonidet P40 supplemented with 1 mmol/L dithiothreitol, 10 mg/mL aprotinin, 10 mg/mL leupeptin, 1 mmol/L phenylmethylsulfonyl fluoride, 1 mmol/L Na3VO4, and 1 mmol/L sodium fluoride. Lysates were clarified by centrifugation and separated on sodium dodecyl sulfate–polyacrylamide gel electrophoresis. Blots were incubated with antibodies against p-p38 (1:1000, #4511S; Cell Signalling Technology, Danvers, MA), p38 (#sc-7972), phosphorylated extracellular signal–regulated kinase-1/2 (#sc-7383), phosphorylated c-Jun N-terminal kinase (#sc-6254) (1:500; all from Santa Cruz Biotechnology), and β-actin antibody (1:5000, #A544; Sigma), followed by a secondary antibody conjugated to horseradish peroxidase (1:20,000; Dako, Santa Clara, CA).

Histopathologic Scoring and Immunohistochemistry

Cryosections of colon and ileum samples were stained with H&E and scored in blinded fashion on the basis of changes of the epithelium and cell infiltration, as previously described.[51] Cryosections of colon specimens were stained with rabbit anti-cleaved caspase-3 antibody (1:150, #9661S; Cell Signalling Technology) and positive cells were visualized using MACH4 Universal Horseradish-Peroxidase Polymer kit with 3,3′-diaminobenzidine tetra hydrochloride (#M4BD534G; Biocare Medical, Pacheco, CA).

Immunofluorescence and Periodic Acid-Schiff–Alcian Blue Staining

Cryosections of colon were placed in methanol–Carnoy's fixative solution (60% methanol, 30% chloroform, 10% glacial acetic acid) for 2 hours at room temperature for Muc-2 detection or in PFA 4% for 10 minutes at room temperature for p-p38 staining. Sections then were washed in PBS 1 time and permeabilized with 0.1% Triton X-100 for 20 minutes. Blocking procedure (bovine serum albumin 1%, Tween 0.1%, glycine 2%) was performed for 1 hour at room temperature and rabbit primary antibody against Muc-2 (1:100, #sc-15334; Santa Cruz Biotechnology), rabbit primary antibody against p-p38 (1:100, #4511S; Cell Signalling Technology), and O-linked sugar residues (1:500, lectin from Dolichos biflorus [horse gram], #L6533; Sigma) were incubated overnight at 4°C. After washing with PBS 1 time, the secondary antibody goat anti-rabbit Alexa 488 (1:2000, #A11008; Invitrogen) and streptavidin Alexa 568 (1:2500, #S11226; Thermo Fisher Scientific) were applied for 2 hours at room temperature. Slides were washed with PBS 1 time and mounted using Prolong gold antifade reagent with 4′,6-diamidino-2-phenylindole (#P36931; Invitrogen) and analyzed by a Leica DMI4000 B microscope with Leica application suite software (V4.6.2). To visualize goblet cells, cryosections of colon samples were placed in methanol–Carnoy's fixative solution for 2 hours at room temperature and stained with the periodic acid-Schiff/Alcian blue stain kit (#04-163802; Bio-Optica, Milan, Italy).

Microbiota Analysis by 16S Ribosomal RNA Gene Sequencing

16S Ribosomal RNA gene sequence analysis was performed by Polo d'Innovazione di Genomica, Genetica e Biologia (Siena, Italy) using genomic DNA extracted from colon biopsy specimens. The libraries were prepared in accordance with the Illumina 16S Metagenomic Sequencing Library Preparation Guide (part # 15044223 Rev. B) and the Nextera XT Index Kit. PCR was performed to amplify template from the DNA samples using region of interest–specific primers (16S V4 region) with overhang adapters attached. A first purification step used AMPure XP beads to purify the 16S amplicon from free primers and primer-dimers.

A second PCR step attached dual indices and Illumina sequencing adapters using the Nextera XT Index Kit. Libraries were validated using the Agilent 2100 Bioanalyzer to check size distribution. Indexed DNA libraries were normalized to 4 nmol/L and then pooled in equal volumes. The pool was loaded at a concentration of 9 pmol/L onto an Illumina Flowcell v2 with 20% of Phix control. The samples then were sequenced using the Illumina MiSeq, 2 × 250 bp paired end run. Quality control was performed using the FastQC tool and the Trimmomatic software package was used. Sequenced paired-end reads were merged to reconstruct the original full-length 16S amplicons with PEAR software. All amplicons with sequence similarity higher than 97% were grouped together and a representative was chosen as input for the taxonomy annotation and building the OTU table. Sequences were searched for matching in the SILVA taxonomy database (v128) using the open-reference OTU picking algorithm. The resulting OTU table was encoded in Biological observation Matrix format (http://biom-format.org/). The α-diversity (within sample) was investigated by means of 3 different indexes: Shannon, Simpson, and Fisher α index. Sample richness was investigated through Chao and phylogenetic diversity estimators. β-diversity was quantified using both OTU- and phylogenetic-based methods. The data set has been deposited in the Sequence Read Archive (accession no. SRP155816, https://www.ncbi.nlm.nih.gov/sra/SRP155816).

Overnight Fasting Blood Glucose Measurement

Mice were exposed to drinking water supplemented with 5% MDX for 10 weeks. After a 15-hour fast, baseline blood glucose levels were measured using the One touch Verio Flex Glucose Meter and expressed as mg/dL.

Statistical Analysis

Parametric data were analyzed using the 2-tailed Student *t* test for comparison between 2 groups or 1-way analysis of variance followed by the Bonferroni post hoc test for multiple comparisons. Nonparametric data were analyzed using the Mann–Whitney *U* test for comparison between 2 groups or the Kruskal–Wallis test for multiple comparisons. Significance was defined as a *P* value less than .05.

References

1. Abraham C, Cho JH. Inflammatory bowel disease. N Engl J Med 2009;361:2066–2078.
2. Bouma G, Strober W. The immunological and genetic basis of inflammatory bowel disease. Nat Rev Immunol 2003;3:521–533.
3. Jostins L, Ripke S, Weersma RK, Duerr RH, McGovern DP, Hui KY, Lee JC, Schumm LP, Sharma Y, Anderson CA, Essers J, Mitrovic M, Ning K, Cleynen I, Theatre E, Spain SL, Raychaudhuri S, Goyette P, Wei Z, Abraham C, Achkar JP, Ahmad T, Amininejad L, Ananthakrishnan AN, Andersen V, Andrews JM, Baidoo L, Balschun T, Bampton PA, Bitton A, Boucher G, Brand S, Buning C, Cohain A, Cichon S, D'Amato M, De Jong D, Devaney KL, Dubinsky M, Edwards C, Ellinghaus D, Ferguson LR, Franchimont D, Fransen K, Gearry R, Georges M, Gieger C, Glas J, Haritunians T, Hart A, Hawkey C, Hedl M, Hu X, Karlsen TH, Kupcinskas L, Kugathasan S, Latiano A, Laukens D, Lawrance IC, Lees CW, Louis E, Mahy G, Mansfield J, Morgan AR, Mowat C, Newman W, Palmieri O, Ponsioen CY, Potocnik U, Prescott NJ, Regueiro M, Rotter JI, Russell RK, Sanderson JD, Sans M, Satsangi J, Schreiber S, Simms LA, Sventoraityte J, Targan SR, Taylor KD, Tremelling M, Verspaget HW, De Vos M, Wijmenga C, Wilson DC, Winkelmann J, Xavier RJ, Zeissig S, Zhang B, Zhang CK, Zhao H, International IBDGC, Silverberg MS, Annese V, Hakonarson H, Brant SR, Radford-Smith G, Mathew CG, Rioux JD, Schadt EE, Daly MJ, Franke A, Parkes M, Vermeire S, Barrett JC, Cho JH. Host-microbe interactions have shaped the genetic architecture of inflammatory bowel disease. Nature 2012;491:119–124.
4. Li X, Sundquist J, Hemminki K, Sundquist K. Risk of inflammatory bowel disease in first- and second-generation immigrants in Sweden: a nationwide follow-up study. Inflamm Bowel Dis 2011;17:1784–1791.
5. Molodecky NA, Soon IS, Rabi DM, Ghali WA, Ferris M, Chernoff G, Benchimol EI, Panaccione R, Ghosh S, Barkema HW, Kaplan GG. Increasing incidence and prevalence of the inflammatory bowel diseases with time, based on systematic review. Gastroenterology 2012;142:46–54 e42, quiz e30.
6. Probert CS, Jayanthi V, Hughes AO, Thompson JR, Wicks AC, Mayberry JF. Prevalence and family risk of ulcerative colitis and Crohn's disease: an epidemiological study among Europeans and south Asians in Leicestershire. Gut 1993;34:1547–1551.
7. Shoda R, Matsueda K, Yamato S, Umeda N. Epidemiologic analysis of Crohn disease in Japan: increased dietary intake of n-6 polyunsaturated fatty acids and animal protein relates to the increased incidence of Crohn disease in Japan. Am J Clin Nutr 1996;63:741–745.
8. Ananthakrishnan AN, Khalili H, Konijeti GG, Higuchi LM, de Silva P, Fuchs CS, Willett WC, Richter JM, Chan AT. Long-term intake of dietary fat and risk of ulcerative colitis and Crohn's disease. Gut 2014;63:776–784.
9. Khalili H, Ananthakrishnan AN, Konijeti GG, Higuchi LM, Fuchs CS, Richter JM, Chan AT. Measures of obesity and risk of Crohn's disease and ulcerative colitis. Inflamm Bowel Dis 2015;21:361–368.
10. Lewis JD, Abreu MT. Diet as a trigger or therapy for inflammatory bowel diseases. Gastroenterology 2017;152:398–414 e6.
11. Racine A, Carbonnel F, Chan SS, Hart AR, Bueno-de-Mesquita HB, Oldenburg B, van Schaik FD, Tjonneland A, Olsen A, Dahm CC, Key T, Luben R, Khaw KT, Riboli E, Grip O, Lindgren S, Hallmans G, Karling P, Clavel-Chapelon F, Bergman MM, Boeing H, Kaaks R, Katzke VA, Palli D, Masala G, Jantchou P, Boutron-Ruault MC. Dietary patterns and risk of inflammatory bowel disease in Europe: results from the EPIC Study. Inflamm Bowel Dis 2016;22:345–354.

12. Devkota S, Wang Y, Musch MW, Leone V, Fehlner-Peach H, Nadimpalli A, Antonopoulos DA, Jabri B, Chang EB. Dietary-fat-induced taurocholic acid promotes pathobiont expansion and colitis in Il10-/- mice. Nature 2012;487:104–108.
13. Martinez-Medina M, Denizot J, Dreux N, Robin F, Billard E, Bonnet R, Darfeuille-Michaud A, Barnich N. Western diet induces dysbiosis with increased E coli in CEABAC10 mice, alters host barrier function favouring AIEC colonisation. Gut 2014;63:116–124.
14. Gulhane M, Murray L, Lourie R, Tong H, Sheng YH, Wang R, Kang A, Schreiber V, Wong KY, Magor G, Denman S, Begun J, Florin TH, Perkins A, Cuiv PO, McGuckin MA, Hasnain SZ. High fat diets induce colonic epithelial cell stress and inflammation that is reversed by IL-22. Sci Rep 2016;6:28990.
15. Monteleone I, Marafini I, Dinallo V, Di Fusco D, Troncone E, Zorzi F, Laudisi F, Monteleone G. Sodium chloride-enriched diet enhanced inflammatory cytokine production and exacerbated experimental colitis in mice. J Crohns Colitis 2017;11:237–245.
16. Tubbs AL, Liu B, Rogers TD, Sartor RB, Miao EA. Dietary salt exacerbates experimental colitis. J Immunol 2017; 199:1051–1059.
17. Desai MS, Seekatz AM, Koropatkin NM, Kamada N, Hickey CA, Wolter M, Pudlo NA, Kitamoto S, Terrapon N, Muller A, Young VB, Henrissat B, Wilmes P, Stappenbeck TS, Nunez G, Martens EC. A dietary fiber-deprived gut microbiota degrades the colonic mucus barrier and enhances pathogen susceptibility. Cell 2016; 167:1339–1353 e21.
18. Mastrodonato M, Mentino D, Portincasa P, Calamita G, Liquori GE, Ferri D. High-fat diet alters the oligosaccharide chains of colon mucins in mice. Histochem Cell Biol 2014;142:449–459.
19. Chassaing B, Koren O, Goodrich JK, Poole AC, Srinivasan S, Ley RE, Gewirtz AT. Dietary emulsifiers impact the mouse gut microbiota promoting colitis and metabolic syndrome. Nature 2015;519:92–96.
20. Nickerson KP, Homer CR, Kessler SP, Dixon LJ, Kabi A, Gordon IO, Johnson EE, de la Motte CA, McDonald C. The dietary polysaccharide maltodextrin promotes Salmonella survival and mucosal colonization in mice. PLoS One 2014;9:e101789.
21. Nickerson KP, McDonald C. Crohn's disease-associated adherent-invasive Escherichia coli adhesion is enhanced by exposure to the ubiquitous dietary polysaccharide maltodextrin. PLoS One 2012;7:e52132.
22. Suez J, Korem T, Zeevi D, Zilberman-Schapira G, Thaiss CA, Maza O, Israeli D, Zmora N, Gilad S, Weinberger A, Kuperman Y, Harmelin A, Kolodkin-Gal I, Shapiro H, Halpern Z, Segal E, Elinav E. Artificial sweeteners induce glucose intolerance by altering the gut microbiota. Nature 2014;514:181–186.
23. Swidsinski A, Ung V, Sydora BC, Loening-Baucke V, Doerffel Y, Verstraelen H, Fedorak RN. Bacterial overgrowth and inflammation of small intestine after carboxymethylcellulose ingestion in genetically susceptible mice. Inflamm Bowel Dis 2009;15:359–364.
24. Thymann T, Moller HK, Stoll B, Stoy AC, Buddington RK, Bering SB, Jensen BB, Olutoye OO, Siggers RH, Molbak L, Sangild PT, Burrin DG. Carbohydrate maldigestion induces necrotizing enterocolitis in preterm pigs. Am J Physiol Gastrointest Liver Physiol 2009; 297:G1115–G1125.
25. Chassaing B, Srinivasan G, Delgado MA, Young AN, Gewirtz AT, Vijay-Kumar M. Fecal lipocalin 2, a sensitive and broadly dynamic non-invasive biomarker for intestinal inflammation. PLoS One 2012;7:e44328.
26. Tsuru A, Fujimoto N, Takahashi S, Saito M, Nakamura D, Iwano M, Iwawaki T, Kadokura H, Ron D, Kohno K. Negative feedback by IRE1beta optimizes mucin production in goblet cells. Proc Natl Acad Sci U S A 2013; 110:2864–2869.
27. Perez-Vilar J, Hill RL. The structure and assembly of secreted mucins. J Biol Chem 1999;274:31751–31754.
28. Heazlewood CK, Cook MC, Eri R, Price GR, Tauro SB, Taupin D, Thornton DJ, Png CW, Crockford TL, Cornall RJ, Adams R, Kato M, Nelms KA, Hong NA, Florin TH, Goodnow CC, McGuckin MA. Aberrant mucin assembly in mice causes endoplasmic reticulum stress and spontaneous inflammation resembling ulcerative colitis. PLoS Med 2008;5:e54.
29. Han J, Lee JD, Bibbs L, Ulevitch RJ. A MAP kinase targeted by endotoxin and hyperosmolarity in mammalian cells. Science 1994;265:808–811.
30. Itoh T, Yamauchi A, Miyai A, Yokoyama K, Kamada T, Ueda N, Fujiwara Y. Mitogen-activated protein kinase and its activator are regulated by hypertonic stress in Madin-Darby canine kidney cells. J Clin Invest 1994; 93:2387–2392.
31. Robinson AM, Rahman AA, Carbone SE, Randall-Demllo S, Filippone R, Bornstein JC, Eri R, Nurgali K. Alterations of colonic function in the Winnie mouse model of spontaneous chronic colitis. Am J Physiol Gastrointest Liver Physiol 2017;312:G85–G102.
32. Van der Sluis M, De Koning BA, De Bruijn AC, Velcich A, Meijerink JP, Van Goudoever JB, Buller HA, Dekker J, Van Seuningen I, Renes IB, Einerhand AW. Muc2-deficient mice spontaneously develop colitis, indicating that MUC2 is critical for colonic protection. Gastroenterology 2006;131:117–129.
33. Velcich A, Yang W, Heyer J, Fragale A, Nicholas C, Viani S, Kucherlapati R, Lipkin M, Yang K, Augenlicht L. Colorectal cancer in mice genetically deficient in the mucin Muc2. Science 2002;295:1726–1729.
34. Martino MB, Jones L, Brighton B, Ehre C, Abdulah L, Davis CW, Ron D, O'Neal WK, Ribeiro CM. The ER stress transducer IRE1beta is required for airway epithelial mucin production. Mucosal Immunol 2013; 6:639–654.
35. Lee JC, Young PR. Role of CSB/p38/RK stress response kinase in LPS and cytokine signaling mechanisms. J Leukoc Biol 1996;59:152–157.
36. Geiger PC, Wright DC, Han DH, Holloszy JO. Activation of p38 MAP kinase enhances sensitivity of muscle glucose transport to insulin. Am J Physiol Endocrinol Metab 2005;288:E782–E788.

37. Guo LX, Xie H. Differential phosphorylation of p38 induced by apoptotic and anti-apoptotic stimuli in murine hepatocytes. World J Gastroenterol 2005;11:1345–1350.
38. Liang KC, Lee CW, Lin WN, Lin CC, Wu CB, Luo SF, Yang CM. Interleukin-1beta induces MMP-9 expression via p42/p44 MAPK, p38 MAPK, JNK, and nuclear factor-kappaB signaling pathways in human tracheal smooth muscle cells. J Cell Physiol 2007;211:759–770.
39. Kim SJ, Ko WK, Jo MJ, Arai Y, Choi H, Kumar H, Han IB, Sohn S. Anti-inflammatory effect of tauroursodeoxycholic acid in RAW 264.7 macrophages, bone marrow-derived macrophages, BV2 microglial cells, and spinal cord injury. Sci Rep 2018;8:3176.
40. Wang W, Zhao J, Gui W, Sun D, Dai H, Xiao L, Chu H, Du F, Zhu Q, Schnabl B, Huang K, Yang L, Hou X. Tauroursodeoxycholic acid inhibits intestinal inflammation and barrier disruption in mice with non-alcoholic fatty liver disease. Br J Pharmacol 2018;175:469–484.
41. Eri RD, Adams RJ, Tran TV, Tong H, Das I, Roche DK, Oancea I, Png CW, Jeffery PL, Radford-Smith GL, Cook MC, Florin TH, McGuckin MA. An intestinal epithelial defect conferring ER stress results in inflammation involving both innate and adaptive immunity. Mucosal Immunol 2011;4:354–364.
42. Ruiz PA, Moron B, Becker HM, Lang S, Atrott K, Spalinger MR, Scharl M, Wojtal KA, Fischbeck-Terhalle A, Frey-Wagner I, Hausmann M, Kraemer T, Rogler G. Titanium dioxide nanoparticles exacerbate DSS-induced colitis: role of the NLRP3 inflammasome. Gut 2017;66:1216–1224.
43. Johansson ME, Larsson JM, Hansson GC. The two mucus layers of colon are organized by the MUC2 mucin, whereas the outer layer is a legislator of host-microbial interactions. Proc Natl Acad Sci U S A 2011;108(Suppl 1):4659–4665.
44. Johansson ME, Phillipson M, Petersson J, Velcich A, Holm L, Hansson GC. The inner of the two Muc2 mucin-dependent mucus layers in colon is devoid of bacteria. Proc Natl Acad Sci U S A 2008;105:15064–15069.
45. Johansson ME, Sjovall H, Hansson GC. The gastrointestinal mucus system in health and disease. Nat Rev Gastroenterol Hepatol 2013;10:352–361.
46. Johansson ME, Gustafsson JK, Holmen-Larsson J, Jabbar KS, Xia L, Xu H, Ghishan FK, Carvalho FA, Gewirtz AT, Sjovall H, Hansson GC. Bacteria penetrate the normally impenetrable inner colon mucus layer in both murine colitis models and patients with ulcerative colitis. Gut 2014;63:281–291.
47. Bergstrom KS, Kissoon-Singh V, Gibson DL, Ma C, Montero M, Sham HP, Ryz N, Huang T, Velcich A, Finlay BB, Chadee K, Vallance BA. Muc2 protects against lethal infectious colitis by disassociating pathogenic and commensal bacteria from the colonic mucosa. PLoS Pathog 2010;6:e1000902.
48. Kissoon-Singh V, Moreau F, Trusevych E, Chadee K. Entamoeba histolytica exacerbates epithelial tight junction permeability and proinflammatory responses in Muc2(-/-) mice. Am J Pathol 2013;182:852–865.
49. Chassaing B, Van de Wiele T, De Bodt J, Marzorati M, Gewirtz AT. Dietary emulsifiers directly alter human microbiota composition and gene expression ex vivo potentiating intestinal inflammation. Gut 2017;66:1414–1427.
50. Monteleone I, Federici M, Sarra M, Franze E, Casagrande V, Zorzi F, Cavalera M, Rizzo A, Lauro R, Pallone F, MacDonald TT, Monteleone G. Tissue inhibitor of metalloproteinase-3 regulates inflammation in human and mouse intestine. Gastroenterology 2012;143:1277–1287 e1-4.
51. Dohi T, Ejima C, Kato R, Kawamura YI, Kawashima R, Mizutani N, Tabuchi Y, Kojima I. Therapeutic potential of follistatin for colonic inflammation in mice. Gastroenterology 2005;128:411–423.

Received March 6, 2018. Accepted September 4, 2018.

Correspondence
Address correspondence to: Giovanni Monteleone, MD, Department of Systems Medicine, University of Rome Tor Vergata, Via Montpellier 1, 00133 Rome, Italy. e-mail: gi.monteleone@uniroma2.it; fax: (39) 06-72596391.

Acknowledgments
The authors thank V. Iebba (Department of Public Health and Infectious Diseases, Institute Pasteur Cenci Bolognetti Foundation, University of Rome La Sapienza) and S. Barbaliscia (Department of Experimental Medicine and Surgery, University of Rome Tor Vergata) for assistance in microbiota analysis, and M. Levrero (Department of Internal Medicine, University of Rome La Sapienza) for data discussion.

Author contributions
F. Laudisi was responsible for the study concept and design, technical and material support, acquisition of data, analysis and interpretation of data, drafting the manuscript, and statistical analysis; D. Di Fusco was responsible for the analysis and interpretation of data, acquisition of data, and technical and material support; V. Dinallo, A. Di Grazia, I. Marafini, A. Colantoni, A. Ortenzi, M. Mavilio, and F. Guerrieri were responsible for technical and material support; C. Stolfi was responsible for the analysis and interpretation of data, and technical and material support; C. Alteri was responsible for the interpretation of data and technical and material support; F. Ceccherini-Silberstein was responsible for the analysis and interpretation of data and critical revision of the manuscript; M. Federici and T. T. MacDonald were responsible for critical revision of the manuscript; I. Monteleone was responsible for the analysis and interpretation of data and critical revision of the manuscript; and Giovanni Monteleone was responsible for the study concept and design, analysis and interpretation of data, and drafting and critical revision of the manuscript. All authors had access to all data and reviewed and approved the final manuscript.

Conflicts of interest
The authors disclose no conflicts.

Funding
This work was supported in part by the Italian Ministry of Instruction, University and Research (Bandiera InterOmics Protocollo PB05 1°).